Role of the C-Terminal Tyrosine of Ferredoxin-Nicotinamide Adenine Dinucleotide Phosphate Reductase in the Electron Transfer Processes with Its Protein Partners Ferredoxin and Flav...

ARTICLE *in* BIOCHEMISTRY · JUNE 2004

Impact Factor: 3.02 · DOI: 10.1021/bi049858h · Source: PubMed

Role of the C-Terminal Tyrosine of Ferredoxin-Nicotinamide Adenine Dinucleotide Phosphate Reductase in the Electron Transfer Processes with Its Protein Partners Ferredoxin and Flavodoxin†

Isabel Nogués,‡,§ Jesús Tejero,‡,§ John K. Hurley,|| Darío Paladini,⊥ Susana Frago,‡ Gordon Tollin,|| Stephen G. Mayhew,▽ Carlos Gómez-Moreno,‡ Eduardo A. Ceccarelli,⊥ Néstor Carrillo,⊥ and Milagros Medina*,‡

Departamento de Bioquímica y Biología Molecular y Celular and Biocomputation and Complex Systems Physics Institute, Facultad de Ciencias, Universidad de Zaragoza, 50009 Zaragoza, Spain, Molecular Biology Division, IBR CONICET-Universidad Nacional de Rosario, Rosario, Argentina, Department of Biochemistry, Conway Institute for Biomolecular and Biomedical Research, University College Dublin, Belfield, Dublin, Ireland, and Department of Biochemistry and Molecular Biophysics, University of Arizona, Tucson, Arizona 85721

Received January 19, 2004; Revised Manuscript Received March 11, 2004

ABSTRACT: The catalytic mechanism proposed for ferredoxin-$NADP^+$ reductase (FNR) is initiated by reduction of its flavin adenine dinucleotide (FAD) cofactor by the obligatory one-electron carriers ferredoxin (Fd) or flavodoxin (Fld) in the presence of oxidized nicotinamide adenine dinucleotide phosphate ($NADP^+$). The C-terminal tyrosine of FNR, which stacks onto its flavin ring, modulates the enzyme affinity for $NADP^+$/H, being removed from this stacking position during turnover to allow productive docking of the nicotinamide and hydride transfer. Due to its location at the substrate-binding site, this residue might also affect electron transfer between FNR and its protein partners. We therefore studied the interactions and electron-transfer properties of FNR proteins mutated at their C-termini. The results obtained with the homologous reductases from pea and *Anabaena* PCC7119 indicate that interactions with Fd or Fld are hardly affected by replacement of this tyrosine by tryptophan, phenylalanine, or serine. In contrast, electron exchange is impaired in all mutants, especially in the nonconservative substitutions, without major differences between the eukaryotic and the bacterial FNR. Introduction of a serine residue shifts the flavin reduction potential to less negative values, whereas semiquinone stabilization is severely hampered, introducing further constraints to the one-electron-transfer processes. Thus, the C-terminal tyrosine of FNR plays distinct and complementary roles during the catalytic cycle, (i) by lowering the affinity for $NADP^+$/H to levels compatible with steady-state turnover, (ii) by contributing to the flavin semiquinone stabilization required for electron splitting, and (iii) by modulating the rates of electron exchange with the protein partners.

Ferredoxin-$NADP^+$ reductase (FNR,[1] EC 1.18.1.2) catalyzes the reduction of $NADP^+$ to NADPH during photosynthesis in higher plants, algae, and cyanobacteria. This flavoprotein contains a single polypeptide chain and a noncovalently bound FAD as the only redox center. FNR accepts one electron from each of two molecules of the one-electron carrier iron sulfur protein ferredoxin (Fd), previously reduced by photosystem I (PSI), and uses these electrons to convert $NADP^+$ into NADPH via hydride transfer from the N-5 atom of the flavin, according to the following reaction (*1*, *2*):

$$2Fd_{rd} + NADP^+ + H^+ \leftrightarrow 2Fd_{ox} + NADPH \quad (1)$$

In the case of several algae and cyanobacteria, particularly when they are grown in a low-iron medium, an FMN-containing flavodoxin (Fld) can replace Fd as electron donor to FNR (*3*), cycling between the fully reduced and the semiquinone states, to provide the NADPH necessary for CO_2 assimilation during photosynthesis. The reaction depicted in eq 1 reflects the ability of the flavin cofactor of FNR to split electrons between obligatory one- and two-electron carriers (*1*, *4*). The study of the FNR catalytic mechanism is important not only due to its intrinsic biological relevance but also because the three-dimensional structure of the protein has been shown to be the prototype for a large family of

† This work has been supported by Comisión Interministerial de Ciencia y Tecnología (CICYT, Grants BIO2000-1259 and BIO2003-00627 to C.G.-M. and Grant BQU2001-2520 to M.M.), by CONSI+D (DGA, Grant P006/2000 to M.M.), by CONICET and ANPCyT (Argentina, to N.C. and E.C.), and by the U.S. National Institutes of Health (DK15057 to G.T.).

* To whom correspondence should be addressed. Fax: +34976762123. Phone: +34976762476. E-mail: mmedina@unizar.es.

‡ Universidad de Zaragoza.

§ These authors have contributed equally to the paper.

|| University of Arizona.

⊥ IBR CONICET-Universidad Nacional de Rosario.

▽ University College Dublin.

[1] Abbreviations: Cb5R, cytochrome b_5 reductase; CYP450R, cytochrome P450 reductase; EDTA, ethylenediaminetetraacetic acid; ET, electron transfer; FAD, flavin adenine dinucleotide; Fd, ferredoxin; Fd_{ox} [Fd_{rd}], ferredoxin in the oxidized [reduced] state; Fld, flavodoxin; Fld_{ox} [Fld_{rd}, Fld_{sq}], flavodoxin in the oxidized [reduced, semiquinone] state; FMN, flavin mononucleotide; FNR, ferredoxin-$NADP^+$ reductase; FNR_{ox} [FNR_{rd}, FNR_{sq}], ferredoxin-$NADP^+$ reductase in the oxidized [reduced, semiquinone] state; dRf, 5-deazariboflavin; K_d, dissociation constant; k_{et}, first-order electron-transfer rate constant; k_{ap}, apparent rate constant; k_{obs}, pseudo-first-order rate constant; $NADP^+$ [NADPH], nicotinamide adenine dinucleotide phosphate in the oxidized [reduced] state; NOS, nitric oxide synthase; NR, nitrate reductase; PDR, phthalate dioxygenase reductase; PSI, photosystem I; SiR, sulfite reductase; SQ, semiquinone; WT, wild type.

10.1021/bi049858h CCC: $27.50
Published on Web 04/27/2004

flavin-dependent oxidoreductases that function as transducers between nicotinamide dinucleotides and different one-electron carriers (*5*−*8*). The FNR molecule consists of two domains. The N-terminal FAD binding domain is made up of a scaffold of six antiparallel strands arranged in two perpendicular β-sheets, whereas the $NADP^+$ binding domain consists of a core of five parallel β-strands surrounded by seven α-helices. The FAD cofactor is bound to the protein through hydrogen bonds, van der Waals contacts, and stacking interactions. The isoalloxazine ring system, which constitutes the reactive part of FAD, interacts with the aromatic side chains of two Tyr residues (Tyr79 and Tyr303 in *Anabaena* FNR). The edge of the dimethylbenzyl ring, which is putatively involved in intermolecular electron transfer (ET) with the protein partner, is the only part of the flavin isoalloxazine moiety exposed to the solvent. According to the general catalytic mechanism proposed for flavin-dependent enzymes, hydride transfer from reduced FAD to $NADP^+$ must involve previous reduction of the flavin by addition of a proton and an electron to each of the nitrogen atoms at positions 1 and 5. Structures of FNR from different sources in various redox states, with mutations in different key residues, and also in complexes with either Fd or $NADP^+$, have been reported (*8*−*12*). Based on three different binding modes so far reported for the FNR/$NADP^+$ interaction, a mechanism for molecular recognition and complex reorganization that provides the adequate orientation for hydride transfer has been proposed (*12*). This mechanism associates the observed protein structural rearrangements with a change in the bound $NADP^+$ molecule conformation from an extended to a more tight conformation, thus allowing the nicotinamide ring to approach the flavin after displacement of the C-terminal Tyr residue that is stacking on the isoalloxazine ring. A critical component of the proposed mechanism is how this Tyr is removed from its stacking position during turnover to allow the entrance of the nicotinamide. To investigate this, the tyrosine in the pea reductase (Tyr308) has been replaced by Trp, Phe, Gly, and Ser. In most cases, the mutations produced enzyme forms in which the preference for $NADP^+$/H over NAD^+/H was markedly decreased and the affinity for both coenzymes was much higher than that of the wild-type (WT) FNR (*11*, *13*). Moreover, the mutated enzymes showed increased catalytic efficiency with both coenzymes (*13*).

Fast kinetic, binding equilibrium, and steady-state studies have suggested that FNR catalysis must proceed through the formation of a transient ternary complex, with Fd binding to a preformed FNR/$NADP^+$ complex (*14*, *15*). Putative ternary complexes have been modeled (*1*, *12*), based on the FNR/Fd (*9*, *10*) and FNR/$NADP^+$ crystal structures (*11*, *12*). The theoretical structures suggest that $NADP^+$ binding to the reductase leads to rearrangements in the conformation and orientation of some residues, allowing the establishment of new ion pairs between the side chains of FNR and Fd (*12*). Moreover, due to its folded conformation over the flavin ring, the phenol group of the C-terminal Tyr in FNR/Fd is located at the interface between FNR and Fd, with the free α-carboxyl group pointing toward the Fd surface (*9*). Therefore, it is important to determine the role of this residue during ET processes with both redox protein partners, Fd and Fld. In the present study we report the characterization of Fd and Fld interactions and ET with pea and *Anabaena* FNR enzymes mutated at the terminal Tyr.

MATERIALS AND METHODS

Oligonucleotide-Directed Mutagenesis. The design and preparation of the pea FNR variants Tyr308Phe, Tyr308Trp, and Tyr308Ser have been described previously (*11*, *13*). The equivalent site-directed mutants of *Anabaena* PCC 7119 FNR (Tyr303Phe, Tyr303Trp, and Tyr303Ser) were prepared by using as template a construct, pET28-FNR, that contained the *pet*H gene inserted into the *Nco*I and *Hin*dIII sites of pET-28a(+) (Novagen), and the QuikChange mutagenesis kit (Stratagene) with suitable oligonucleotides. Mutations were verified by DNA sequence analysis. The pET28-FNR vectors with the desired mutation were used to transform *Escherichia coli* BL21(DE3) Gold cells (Stratagene).

Protein Purification. E. coli cultures were grown at 30 °C for 24 h without isopropyl β-D-thiogalactoside. The WT and mutated *Anabaena* and pea FNR forms, *Anabaena* Fld and Fd, as well as pea Fd, were isolated by published procedures (*11*, *13*, *16*−*18*).

Spectral Analysis. UV−visible spectra were recorded in a Kontron Uvikon 942 or in a Shimadzu UV-2450 spectrophotometer. Circular dichroism spectra were recorded in a Jasco 710 spectropolarimeter in 1 mM Tris-HCl, pH 8.0 at 25 °C in a 1-cm path length cuvette. FNR concentrations were 0.7 μM for the far-UV and 4 μM for the aromatic and visible regions of the spectrum. The molar absorption coefficient of the bound flavin I band at 459 nm was determined by precipitating the apoprotein with trichloroacetic acid at 4 °C, and separating it from the FAD by centrifugation. The released cofactor was quantitated spectrophotometrically. Protein fluorescence was monitored on a SFM 25 spectrofluorometer from Kontron Instruments. Solutions contained 5 μM protein in 50 mM Tris-HCl, pH 8.0. K_d values and binding energies of the FNR_{ox}/Fd_{ox} and FNR_{ox}/Fld_{ox} complexes were obtained at 25 °C in 50 mM Tris-HCl, pH 8.0, by difference absorption spectroscopy (*16*). Errors in the estimated K_d, $\Delta\epsilon$, and $\Delta G°$ values were ±15%, ±15%, and ±10%, respectively. The FNR-dependent NADPH−cytochrome *c* reductase activity was assayed in 50 mM Tris-HCl, pH 8.0, with either Fd or Fld as electron carrier from FNR_{rd} to cytochrome *c* (*16*). Errors in the estimated values of K_m and k_{cat} were ±15% and ±10%, respectively.

Photoreduction of protein-bound flavin was carried out at 25 °C in an anaerobic cuvette containing 15−25 μM FNR in 50 mM Tris-HCl, pH 8.0, supplemented with 1 mM EDTA and 2 μM dRf to initiate photoreduction of proteins via the highly reductive 5-deazariboflavin radical (dRfH$^\bullet$) (*19*). The following extinction coefficients were used for quantitation of redox species at 458 and 600 nm: FNR_{ox}, 9400 M^{-1} cm^{-1} (*20*) and 200 M^{-1} cm^{-1} (*18*), respectively; FNR_{sq}, 3400 M^{-1} cm^{-1} (spinach enzyme; *15*) and 5000 M^{-1} cm^{-1} (*20*), respectively; FNR_{rd}, 900 M^{-1} cm^{-1} (*20*) and 300 M^{-1} cm^{-1} (*18*), respectively.

Spectroelectrochemistry for the Determination of Oxidoreduction Potentials. Potentiometric titrations of recombinant WT, Tyr303Ser, Tyr303Phe, and Tyr303Trp FNR variants of *Anabaena* FNR, as well as that of FAD, were performed anaerobically with a calomel electrode as reference (*21*). Typical experimental solutions contained 25−40 μM protein, 1−3 μM indicator dyes, 1 μM dRf, and 1 mM EDTA in 50 mM Tris-HCl buffer, pH 8.0, at 25 °C. Indicator dyes benzyl viologen (−348 mV) and methyl viologen (−443

mV) were selected to cover the experimental potential range of each FNR titration, whereas anthraquinone-2-sulfonate (−225 mV) was used for FAD titration. Stepwise FAD or FNR photoreduction was achieved by irradiating the solution (with the cell immersed in ice water) with a 50 W projector bulb for approximately 1 min. After reduction, the cell was placed in a temperature-controlled holder in a Cary 1 spectrophotometer. The solution potential was monitored with a Sycopel Ministat potentiostat. Equilibration of the system was considered established when the measured potential remained stable for 10 min, and the UV−vis spectrum was then recorded. Since the FAD semiquinone is not very stable in these proteins, it was not possible to measure the reduction potentials for the two one-electron steps directly. Values for $E_{ox/rd}$ of the various FNR proteins and FAD were determined according to the Nernst equation:

$$E = E_{ox/rd} + (0.056/n) \log ([ox]/[red]) \qquad (2)$$

where E is the measured equilibrium potential at each point in the titration, n is the number of electrons transferred to the system, and ([ox]/[red]) is the ratio between the redox species at equilibrium, as determined from the absorbance spectrum. Each FNR species displayed two-electron redox behavior on the basis of the slopes of the Nernst plot, ∼30 mV. The reduction potentials are reported versus the standard hydrogen electrode. The error in the E determinations was estimated to be ±3 mV.

Stopped-Flow Kinetic Measurements. Stopped-flow experiments were carried out under anaerobic conditions on an Applied Photophysics SX17.MV spectrophotometer as previously described (*16*). Reduced samples of FNR, Fd, and Fld were prepared by photoreduction with dRf (*16*, *22*). Reactions between FNR and Fld were followed at 600 nm, whereas reactions between FNR and Fd were followed at 507 nm (*16*). Proteins were mixed at a ∼1:1 molar ratio and final concentrations of ∼10 μM. All reactions were carried out in 50 mM Tris-HCl, pH 8.0 at 13 °C. The apparent observed rate constants (k_{ap}) were calculated by fitting the data to mono- or biexponential processes. Errors in their estimated values were ±15%.

Laser-Flash Absorption Spectroscopy. The laser flash photolysis and the photochemical systems that generate reduced protein in situ have been previously described (*16*, *23*, *24*). Samples containing 0.1 mM dRf and 1 mM EDTA in 4 mM potassium phosphate buffer, pH 7.0, were made anaerobic in a long-stem cuvette with 1 cm path length by bubbling H_2O-saturated Ar for 1 h. Microliter volumes of concentrated protein were introduced through a rubber septum with a Hamilton syringe under anaerobic conditions. Generally, 4−10 flashes were averaged. Kinetic traces were analyzed by a computer fitting routine (Kinfit, OLIS, Bogart, GA). Experiments were performed at 25 °C. Errors in the estimated values of the dissociation constants (K_d) of the complexes and the ET rate constants (k_{et}) were ±15% and ±5%, respectively.

RESULTS

Expression and Purification of the FNR Mutants. The expression levels of the *Anabaena* and pea FNR mutants in *E. coli* were similar to those of the recombinant WT enzymes. All reductase variants were obtained in homogeneous form as judged by SDS−polyacrylamide gel electrophoresis. The visible spectra of *Anabaena* Tyr303Trp and Tyr303Ser FNRs indicated that the purified enzymes contained bound $NADP^+$, as already reported for the corresponding pea reductase mutants (*11*). The nucleotide could be efficiently removed by chromatography on a Cibacron-blue matrix.

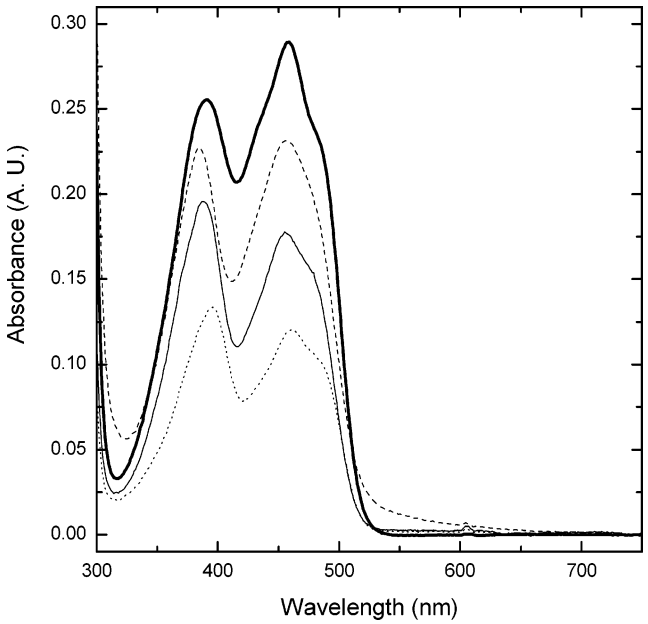

FIGURE 1: Absorption spectra of WT (bold solid line), Tyr303Trp (dashed line), Tyr303Ser (thin solid line), and Tyr303Phe (dotted line) *Anabaena* FNR forms in the visible region. The spectra were recorded in 50 mM Tris-HCl, pH 8.0 at 25 °C. Different protein concentrations were used in order to clarify the figure.

Table 1: UV−Vis Spectral Properties of WT and Mutants of *Anabaena* PCC 7119 FNR_{ox} [a]

FNR	UV max (nm)	band II max (nm)	band I max (nm)	abs ratio II/I	ϵ_I (mM^{-1} cm^{-1})
WT	274	391	459	0.88	9.4
Y303F	274	395	460	1.11	9.1
Y303S	272	389	456	1.09	9.2
Y303W	274	385	456	0.98	9.2

[a] All spectra were recorded in 50 mM Tris-HCl, pH 8.0, at 25 °C.

Spectral Properties. Replacement of the terminal Tyr in *Anabaena* FNR results in small, but significant, changes in the UV−vis absorption properties of the flavin prosthetic group. The absorbance maxima of both transition bands, in the 450 (band I) and 380 (band II) nm regions, were slightly shifted in all the mutants relative to WT FNR (Figure 1, Table 1). Thus, replacement of Tyr303 by a Phe produced small shifts of both transitions to longer wavelengths, whereas introduction of a Trp or a Ser led to a more pronounced displacement of the maxima to shorter wavelengths (Table 1). These shifts presumably aroused from alterations in the isoalloxazine ring environment upon replacement of Tyr303. Thus, substitution of the C-terminal residue by Phe apparently had little effect on the flavin environment, while introduction of Trp or Ser led to a different environment of the isoalloxazine ring. In the case of the Ser mutant, the prosthetic group must display a considerable degree of solvent exposure, as can be observed in the three-dimensional structure reported by Deng et al. (*11*). In addition, replacement of Tyr303 by Trp renders a spectrum with a broad transition that extends beyond 600 nm (Figure 1). A similar transition has been described in an equivalent mutation of

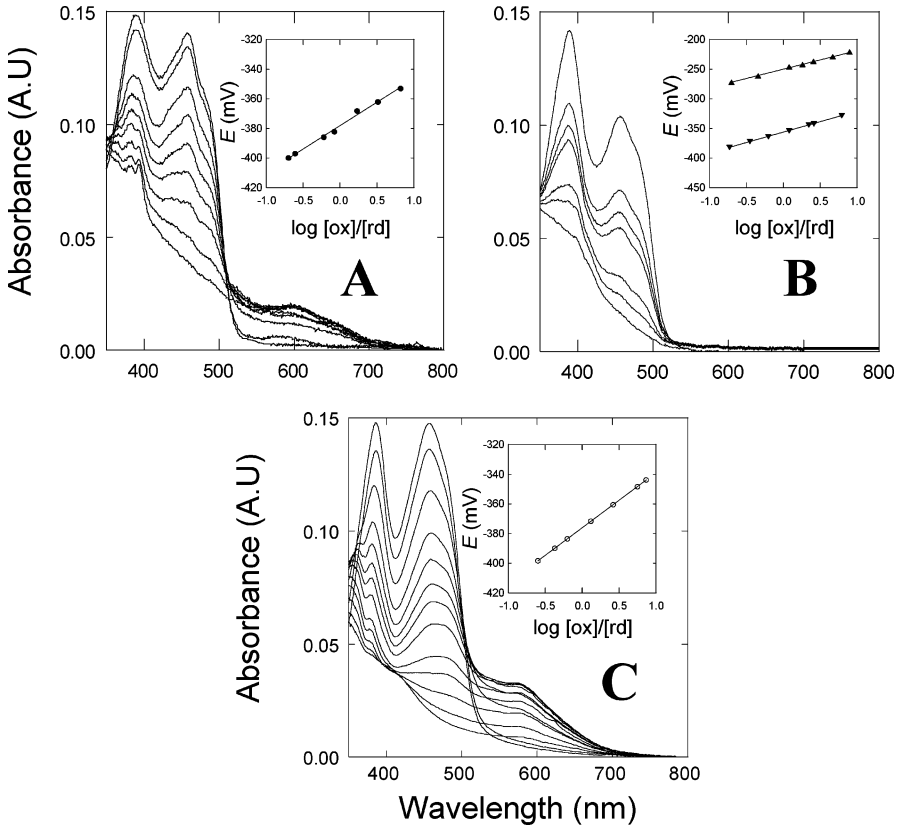

FIGURE 2: Spectra obtained during photoreduction of (A) WT, (B) Tyr303Ser, and (C) Tyr303Trp *Anabaena* FNRs. The insets show the corresponding Nernst plots for WT (●), Tyr303Ser (▲), Tyr303Phe (▼), and Tyr303Trp (○) FNR forms. Measurements were carried out in 50 mM Tris-HCl, pH 8.0 at 25 °C.

flavodoxin and was attributed to a charge-transfer complex between the Trp indole ring and the flavin (*25*). Changes in the relative absorptivity of both flavin transition bands were observed in all cases, with an increase in the absorptivity of transition II with respect to transition I (Table 1).

The FAD fluorescence of the Tyr303Phe and Tyr303Trp reductases was essentially the same as that of the WT enzyme, around 4% of the free FAD fluorescence. Replacement of Tyr303 by Ser slightly increased the FAD fluorescence to 10% of that of free flavin (data not shown). It is noteworthy that addition of $NADP^+$ to this FNR mutant decreased the FAD fluorescence below that of the WT enzyme, suggesting that the nicotinamide of $NADP^+$ quenches the flavin fluorescence, as does the aromatic residue at position 303 in the other forms of FNR. The circular dichroism spectra of the different FNR mutants were similar to that of the WT enzyme (data not shown). Only slight shifts of the peak positions and small changes in the relative molar ellipticities of the different bands were observed, which correlate with the changes found in the absorption spectra. In conclusion, this characterization indicates small spectral perturbations that are likely to be caused by subtle changes in the microenvironment of the isoalloxazine ring. Moreover, despite the reported fact that it is easier to remove a Trp than a Tyr at the C-terminus by the $NADP^+$/H nicotinamide ring (*11*), analysis of the three-dimensional structures reported for the equivalent mutants in pea FNR suggest that flavin exposure to the solvent in the Tyr303Trp FNR is similar to that of the WT, and only replacement by a Ser leads to a considerable increase in the flavin accessibility to the solvent.

Photoreduction of Anabaena FNR Mutants and Determination of Their Oxidation−Reduction Potentials. Photoreduction of the various FNR forms allowed an accurate quantitation of the amount of total neutral flavin semiquinone (SQ) stabilized during reduction (*19*). Our data indicate that while the WT and the Tyr303Phe and Tyr303Trp mutants of *Anabaena* FNR accumulate maxima of 27%, 35% and 27%, respectively, of the total flavin as SQ, almost no absorbance changes attributable to the SQ could be detected in the case of Tyr303Ser FNR, leading to the estimate that the maximum of this species accumulated during reduction must be below 1.2% (Figure 2, Table 2).

Table 2: Midpoint Reduction Potentials of WT and Mutants of *Anabaena* FNR[a]

FNR	$E_{ox/rd}$ (mV)	$E_{ox/sq}$ [a] (mV)	$E_{sq/rd}$ [a] (mV)	% SQ
WT	−374	−385	−371	27
Y303F	−356	−358	−354	35
Y303S	−250	−338	−162	1.2
Y303W	−376	−383	−369	27
FAD	−241	−373	−109	0.2[b]

[a] These values were calculated from eqs 3 and 4 as described in the text. [b] Data from Faro et al. (*19*).

Values for the reduction potential of the two-electron reduction ($E_{ox/rd}$) of each enzyme form were determined experimentally (Table 2). Where possible (WT FNR and Tyr303Phe and Tyr303Trp FNR mutants), the values for $E_{ox/sq}$ and $E_{sq/rd}$ were derived according to eqs 3 and 4, by using the experimentally determined $E_{ox/rd}$ values and the maximum percentage of SQ stabilized by each mutant, as indicated above (*19*, *26*):

$$E_{ox/sq} - E_{sq/rd} = 0.11 \log (2[SQ]/(1 - [SQ])) \quad (3)$$

$$(E_{ox/sq} + E_{sq/rd})/2 = E_{ox/rd} \quad (4)$$

Table 3: Dissociation Constants, Extinction Coefficient Changes, and Free Energies for Complex Formation of Wild-Type and Mutated *Anabaena* PCC 7119 and Pea FNR_{ox} Forms with either Fd_{ox} or Fld_{ox}

FNR	K_d^{Fd} (μM)	$\Delta\epsilon^{Fd}$ ($mM^{-1}\,cm^{-1}$)	ΔG^{Fd} (kcal mol^{-1})	K_d^{Fld} (μM)	$\Delta\epsilon^{Fld}$ ($mM^{-1}\,cm^{-1}$)	ΔG^{Fld} (kcal mol^{-1})
			Anabaena FNR			
WT[a]	4.0	2.0	−7.3	3.0	1.4	−7.4
WT/$NADP^+$ [b]	5.1	2.9	−7.2	30.6	2.5	−6.1
Y303F	2.8	2.0	−7.6	8.7	2.5	−6.9
Y303S	0.4	1.4	−8.7	1.0	2.0	−7.8
Y303S/$NADP^+$ [b]	1.18	1.2	−8.2	14.5	2.9	−6.6
Y303W	0.8	2.3	−8.3	*c*	*c*	*c*
			Pea FNR			
WT	4.5	3.9	−7.2			
Y308F	3.8	3.5	−7.3			
Y308S	0.8	0.6	−8.3			
Y308S/$NADP^+$ [b]	2.3	3.2	−7.7			
Y308W	1.0	3.5	−8.1			

[a] Data from Medina et al. (*16*). [b] Parameters for complex formation of the redox protein partners (Fd_{ox}, Fld_{ox}) to the corresponding FNR/$NADP^+$ complexes. [c] Difference spectra were obtained but the experimental data did not fit to the theoretical equation for a 1:1 complex.

Substitution of Tyr303 by Phe shifted $E_{ox/rd}$, $E_{ox/sq}$, and $E_{sq/rd}$ to slightly less negative values (the shifts were +18, +27, and +17 mV, respectively), whereas replacement by Trp had almost no effect on these parameters (−2, +2, and +2 mV, respectively). On the other hand, the midpoint reduction potential calculated from the Nernst plot for the two-electron reduction of Tyr303Ser FNR (inset, Figure 2B) was 124 mV less negative than that of the WT enzyme (Table 2). Due to the lack of SQ stabilization observed for this mutant, it was only possible to calculate reduction potentials for the two independent one-electron processes by assuming an estimated SQ percentage of 1.2%. The resulting values were much closer to the potentials of the free flavin than to those of the other FNR variants (Table 2). Therefore, the data indicate that position 303 in *Anabaena* FNR contributes to the modulation of the redox properties of the flavin ring within the protein environment.

Interaction of FNR_{ox} Forms with Fd_{ox} and Fld_{ox}. To further investigate the effects of mutations at the C-terminal Tyr of FNR on the catalytic mechanism of the flavoenzyme, the interaction of the *Anabaena* and pea mutant reductases with their protein partners, Fd and Fld, was evaluated by difference spectroscopy (*16*). In all cases, the spectral changes produced when FNR_{ox} mutants were titrated with Fd_{ox} or Fld_{ox} were similar to those found for WT FNR_{ox}, and only minor displacements of the minima and maxima were detected, even when Tyr303Ser FNR_{ox} (or Tyr308Ser FNR_{ox}), containing bound $NADP^+$ was used. Although only slight changes were detected in the extinction coefficients for the two protein substrates, a moderate decrease of K_d for both Fd and Fld was indeed observed in the Ser and Trp mutants (Table 3). Difference spectra were obtained for the interaction between *Anabaena* Tyr303Trp FNR_{ox} and Fld_{ox}, but the experimental data did not fit to the theoretical equation for a binary complex with 1:1 stoichiometry, therefore precluding K_d determination. It is interesting to note that prior binding of $NADP^+$ to either WT or Tyr303Ser FNR_{ox} (or to Tyr308Ser pea FNR_{ox}) weakened the subsequent interaction of the corresponding reductases with Fd_{ox} or Fld_{ox} (Table 3).

Steady-State Kinetics. The NADPH-dependent cytochrome *c* reductase activity of the various FNR mutants was also studied with different electron mediators: *Anabaena* Fd and Fld for the cyanobacterial enzyme, pea Fd and *Anabaena* Fld for the plant reductase. The kinetic parameters of WT pea FNR for the reaction with Fld were in the range of those reported for the *Anabaena* enzyme, with a slightly larger k_{cat} and a smaller K_m. The combined effect of both changes led to a moderate increase in the catalytic efficiency of the reaction, relative to the cyanobacterial reductase. Mutation of the C-terminal Tyr had a dramatic effect on the k_{cat} values, whereas considerably smaller effects on the corresponding K_m values were observed (Table 4). Thus, substitution by a Phe in FNR from both species decreased the k_{cat} by 3- to 8-fold for all reactions assayed. Replacement by a Ser produced enzymes that displayed little or no activity in the NADPH−cytochrome *c* reductase assay, whereas introduction of a Trp at this position severely impaired activity, especially when Fd was the electron carrier. Table 4 also shows that K_m values were only slightly affected by the mutations, with the K_m for the Tyr303Phe FNR/Fd interaction undergoing a moderate increase (5-fold higher) with respect to the WT flavoenzyme.

Table 4: Steady-State Kinetic Parameters of WT and Mutated *Anabaena* and Pea FNR Forms in the NADPH-Dependent Cytochrome *c* Reductase Activity with Either Fd or *Anabaena* Fld as Electron Carriers

FNR form	k_{cat}^{Fd} (s^{-1})	K_m^{Fd} (μM)	k_{cat}^{Fd}/K_m^{Fd} ($\mu M^{-1}\,s^{-1}$)	k_{cat}^{Fld} (s^{-1})	K_m^{Fld} (μM)	k_{cat}^{Fld}/K_m^{Fld} ($\mu M^{-1}\,s^{-1}$)
			Anabaena FNR			
WT[a]	200	11	18.2	23.3	33	0.7
Y303F	32.0	51	0.64	7	43	0.17
Y303S	*b*	*b*	*b*	*b*	*b*	*b*
Y303W	1[c]			2.5[c]		
			Pea FNR			
WT	139	6.5	21.3	30.6	16.7	1.8
Y308F	23.9	5.8	4.1	4.0	20.0	0.2
Y308S	7.7	9.0	0.9	*b*	*b*	*b*
Y308W	2.5[c]			8.3	17	0.5

[a] Data from Medina et al. (*16*). [b] No reaction was observed. [c] Only k_{cat} values could be estimated due to the very small extent of reaction observed.

Taking into account the low stabilization of the SQ state by the Tyr303Ser FNR form, which in other FNR mutants has been related to the reduction and reoxidation mechanism (*16*), we assayed the oxidase activity of the *Anabaena* FNR mutants by mixing the different FNR forms with NADPH in the absence of any exogenous electron acceptor and under aerobic conditions. All FNR mutants displayed reoxidation

Table 5: Laser Flash Kinetic Parameters for the Reduction of FNR by Fd[a]

	μ = 100 mM			μ = 375 mM		
FNR form	k (M^{-1} s^{-1})	K_d (μM)	k_{et} (s^{-1})	k (M^{-1} s^{-1})	K_d (μM)	k_{et} (s^{-1})
			Anabaena FNR			
WT		7.6	5500		10	1500
Y303F	0.79×10^8				11.6	2100
Y303S	1.2×10^8				11.6	2500
Y303W	0.43×10^8			9.4×10^6		
			Pea FNR			
WT		20	4000			
Y308F		8.8	1500			
Y308S		20	4000			

[a] The various FNR forms were titrated into solutions containing 30 μM *Anabaena* or pea Fd, respectively.

rates similar to those of the WT enzyme, and only Tyr303Trp reacted slightly faster (data not shown).

Reduction of FNR Mutants Studied by Laser Flash Photolysis. The reduction of the *Anabaena* and pea FNR mutants by laser-generated dRfH$^{\bullet}$ was monitored by the absorbance increase at 600 nm, due to FNR_{sq} formation. Transients were fitted by monoexponential curves, and the calculated rate constants were within a factor of 2 of that of the WT FNR protein (data not shown), consistent with little or no alteration of the FAD reactivity by the mutations. Transient decay curves for the reduction of FNR_{ox} by Fd_{rd} were also monitored at 600 nm. When nonlinear plots of the observed rate constants (k_{obs}) vs FNR concentration were obtained by fitting the flash photolysis kinetic data, the values of K_d for the intermediate Fd_{rd}/FNR_{ox} complex and of k_{et} for the ET process between Fd_{rd} and FNR_{ox} could be calculated (*27*). The results are summarized in Table 5, together with the second-order rate constants for the Fd_{rd}/FNR_{ox} interaction of those mutants for which k_{obs} depended linearly on the FNR concentration.

Figure 3 shows the dependence of k_{obs} on FNR concentration for the ET interaction between Fd_{rd} and the *Anabaena* FNR_{ox} mutants at two different ionic strengths (μ). At μ = 100 mM, the three mutants showed a linear dependence of k_{obs} on enzyme concentration. At low FNR concentrations the k_{obs} values for the mutants were smaller than those obtained for the WT, but they approached the latter values as the enzyme concentrations were raised (Figure 3A). The linear relationship between k_{obs} and enzyme concentration indicates that a stable intermediate complex did not form during the ET process with the mutants or that the K_d values were very large relative to that of the WT. Impairment of the ET was more pronounced when the C-terminal Tyr was replaced by the bulky aromatic residues than by a Ser, although the three FNR forms showed similar binding affinities in the oxidized state (Table 3). At μ = 375 mM, k_{obs} for the Tyr303Phe and Tyr303Ser FNR mutants approached maxima at high concentration of FNR. The K_d values for the intermediate Fd_{rd}/FNR_{ox} complexes for the mutants were similar to those of WT FNR, whereas the k_{et} values were somewhat larger (Table 5). In the case of the Tyr303Trp mutant at μ = 375 mM, k_{obs} still varied linearly with the FNR concentration (Figure 3B), and therefore, values of k_{et} and K_d for the intermediate complex could not be obtained. The reactivity of this mutant was significantly

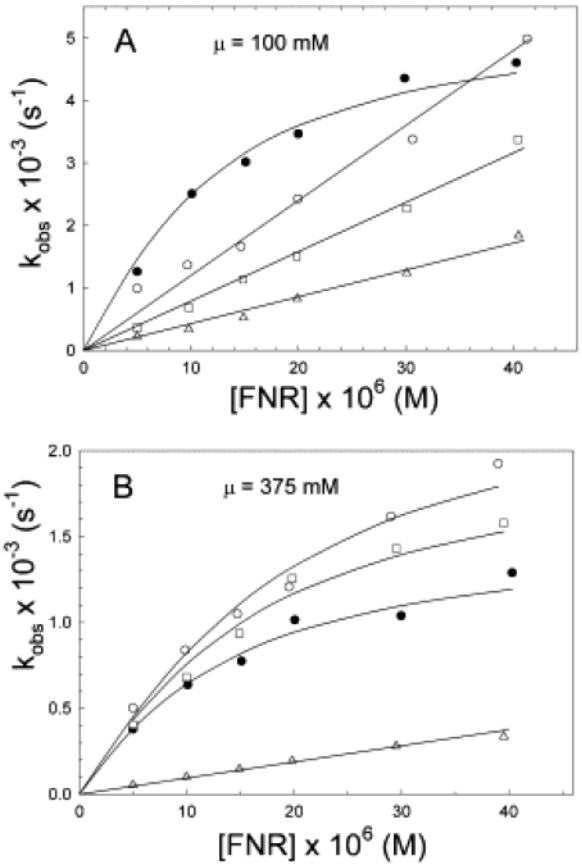

FIGURE 3: Dependence of k_{obs} for Fd_{rd} reoxidation on the concentration of WT (●), Tyr303Ser (○), Tyr303Phe (□), and Tyr303Trp (△) *Anabaena* FNR_{ox} forms at μ = 100 mM (A) and μ = 375 mM (B), obtained by laser flash photolysis. FNR was titrated into solutions containing 30 μM Fd. The monitoring wavelength was 600 nm.

lower than that of the WT FNR and was also decreased with regard to the values at μ = 100 mM (Figure 3).

A biphasic dependence of k_{obs} on μ was observed for *Anabaena* Tyr303Ser and Tyr303Phe FNR mutants (data not shown). Such biphasic behavior has been previously reported in this system and has been interpreted to indicate that the intermediate ET complex formed at low ionic strength is tight but not in an optimal orientation for reaction (*24*, *28*). In contrast, the Tyr303Trp mutant failed to display this biphasic effect in the ionic strength range measured (data not shown). At the physiologically relevant value of μ = 100 mM ($\mu^{1/2} \approx 0.3$), this mutant was substantially hindered in its ET interactions with Fd_{rd}. Thus, placing a Trp residue at positions 303 in *Anabaena* FNR dramatically impairs ET with Fd_{rd}.

The reaction between WT pea FNR_{ox} and pea Fd_{rd} at an ionic strength of 100 mM (Figure 4A) was similar to that of the *Anabaena* system but with slightly smaller k_{obs} values. The rate of FNR reduction by Fd displayed a saturation kinetics for all reductase forms, allowing determination of the dissociation constants for the intermediate FNR_{ox}/Fd_{rd} complexes as well as the corresponding ET rate constants (Table 5). The ionic strength dependence of k_{obs} for the pea proteins was biphasic, showing a maximum at $\mu \approx 0.2$ M for the Tyr308Phe form and at a slightly lower value for the Tyr308Ser reductase. The k_{obs} values for these mutants peaked at about 65% of those obtained with WT FNR (Figure 4B).

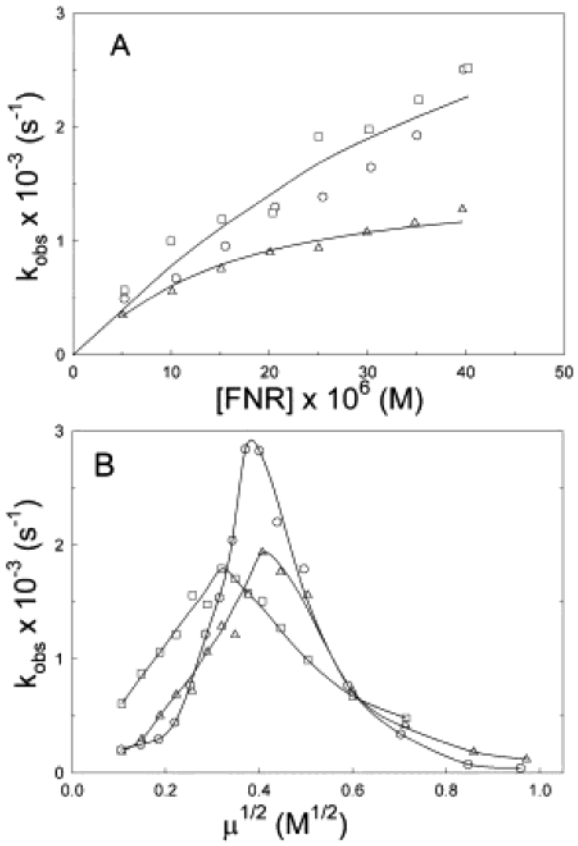

FIGURE 4: Reduction of pea FNR forms by pea Fd. (A) Dependence of k_{obs} values on the concentration of WT (○), Tyr308Ser (□), and Tyr308Phe (△) pea FNR variants at $\mu = 100$ mM. FNR was titrated into solutions containing 30 μM Fd. The monitoring wavelength was 600 nm. (B) Dependence of k_{obs} values on ionic strength for the reduction of WT (○), Tyr308Ser (□), and Tyr308Phe (△) pea FNR forms.

Rapid Reaction Stopped-Flow Studies. Stopped-flow kinetic studies were carried out on the different *Anabaena* and pea FNR mutants to further study the time course of association and ET between FNR and Fd or Fld, in both the oxidized and reduced states (*16*). Reactions between FNR and Fd were followed at 507 nm, an isosbestic point for FNR_{ox} and FNR_{sq} and close to an isosbestic point for FNR_{sq} and FNR_{rd}, an appropriate wavelength to detect both Fd reduction and reoxidation.

It was found that the fully reduced forms of the *Anabaena* FNR mutants did not reduce Fd_{ox} (data not shown). This is in stark contrast to the WT of this FNR, which reduced Fd in a reaction too fast to be followed by stopped-flow spectrophotometry (*16*). Previous stopped-flow studies of the reverse ET process between Fd_{rd} and FNR_{ox} have indicated that the first ET step to produce FNR_{sq} and Fd_{ox} takes place within the instrument dead time (rate constant larger than 1000 s^{-1}) and that the final reaction observed corresponds to the oxidation of a second Fd_{rd} molecule and reduction of FNR_{sq} to FNR_{rd} (*15*, *16*). The different mutants of *Anabaena* FNR were also reduced by Fd_{rd} within the instrument dead time, therefore precluding the estimation of the k_{ap} values (data not shown). These observations confirm the results obtained by laser flash photolysis (Table 5), showing that the expected k_{ap} for ET between Fd_{rd} and *Anabaena* FNR_{ox} mutants at the ionic strength at which stopped-flow experiments were carried out ($\mu = 0.028$ M, $\mu^{1/2} = 0.17$) should be in the same range as that of the reaction with WT FNR.

Electron exchanges between FNR and Fld from *Anabaena* were also analyzed for the FNR mutants from both *Anabaena* and pea. Most reactions were followed at 600 nm to observe production of the semiquinone forms of Fld and FNR. Two phases were detected in the measurements of ET from reduced forms of the Tyr303Phe and Tyr303Trp mutants of *Anabaena* FNR to Fld (data not shown). As was previously reported for the WT of this FNR (*16*), they correspond to the successive transfer of electrons from FNR_{rd} and FNR_{sq} to two different molecules of Fld_{ox}. The k_{ap} values for the reactions of the two FNR mutants were within a factor of 3 of those reported for the WT enzyme. However, a single process, with considerably smaller amplitude and k_{ap} values was observed in the reaction of Tyr303Ser FNR_{rd} mutant (data not shown). A similar study of the reaction of WT pea FNR_{rd} and *Anabaena* Fld_{ox} indicated that, as with *Anabaena* FNR, this reaction also occurred in two phases of similar amplitude with k_{ap} values slightly larger than those observed for WT *Anabaena* FNR (9.2 s^{-1} and 2.3 s^{-1} vs 2.5 s^{-1} and 1.0 s^{-1}). The pea FNR mutants reacted similarly but the amplitudes were only about half those obtained with the WT enzyme. The k_{ap} values obtained for the reaction of the pea Tyr308Trp mutant were similar to those of the WT reductase, while slightly lower values were obtained with the Tyr308Ser and Tyr308Phe mutants (data not shown). The reduction of WT *Anabaena* FNR_{ox} by Fld_{rd} occurs within the instrument dead time (*16*), whereas the corresponding reactions of all *Anabaena* and pea FNR mutants were similarly too fast to be measured.

To determine whether the reoxidation of the fully reduced forms of the *Anabaena* FNR mutants by molecular oxygen proceeds as in the native WT enzyme, the fully reduced mutant reductases were allowed to react with molecular oxygen in the stopped-flow spectrophotometer, and the reactions were monitored at 460 nm (FNR_{ox} formation) and 600 nm (FNR_{sq} formation). The traces obtained for these processes with the Tyr303Phe and Tyr303Trp FNR mutants were similar to those observed for the WT enzyme at both wavelengths (data not shown, but see ref *16*), indicating that reoxidation occurs through the production of the semiquinone as an intermediate. The k_{ap} values for the mutants (5−10 s^{-1} for k_{ap1} and 1−2 s^{-1} for k_{ap2}) were similar to those of the WT. In contrast, very little absorbance change at 600 nm was observed during the reaction of Tyr303Ser FNR_{rd} with oxygen, indicating that this mutant does not stabilize the SQ state during the reaction.

DISCUSSION

Since the first crystal structures of plant FNR became available (*5*), it was evident that the C-terminal Tyr had to play a significant role in the enzyme function. The phenol side chain of this residue stacks coplanar to the isoalloxazine ring system of FAD and needs to be displaced to allow docking of the nicotinamide group of $NADP^+$/H as a mandatory step during catalytic turnover (*5*, *7*, *8*). Further research on pea FNR showed that replacement of this residue by different amino acids leads to drastic alterations in nucleotide binding and catalysis (*11*, *13*). Recent proposals, largely derived from structural studies, suggested that this

Tyr might be involved in the establishment of ternary complexes competent for hydride and electron transfer (*12*, *29*). According to these views, $NADP^+$/H interacts first with FNR in a nonproductive manner through the 2′-P-AMP region. Fd binding might then facilitate displacement of the C-terminal Tyr by nestling the phenol side chain into a hydrophobic pocket of the iron-sulfur protein, favoring nicotinamide docking and establishing a loosely bound complex compatible with turnover (*12*, *29*).

These hypotheses prompted us to probe the effect of site-directed substitutions at the C-terminal position on the interaction and ET with Fd and Fld, the protein electron-transfer partners of FNR. To determine whether the observations are a common feature of eukaryotic and cyanobacterial enzymes, we studied these effects on the homologous reductases from *Anabaena* and pea, enzymes that share 52% sequence identity (*30*). Our data indicate that mutagenesis of Tyr308 in pea FNR and of the equivalent residue, Tyr303, in the *Anabaena* flavoenzyme modifies the flavin environment (and especially when a Ser is introduced in such C-terminal position also the solvent accessibility), the flavin SQ state stabilization, and the redox properties of the enzyme. Such effects might even block some of the electron exchange pathways with Fd. Binding of Fd and Fld was also found to be slightly affected by the mutations (Table 3), again in particular when the terminal Tyr was replaced by a Ser. The data of Table 3 also show that prior binding of $NADP^+$ causes a significant decrease in the affinity of FNR for both electron carrier proteins. These results concur with the negative cooperativity for substrate binding observed with spinach FNR (*14*, *15*). In the plant reductase, this step is required to facilitate product release after electron and hydride transfer. Otherwise, binding of the product would be too strong to be compatible with steady-state catalysis (*15*). The present results are the first demonstration of a similar effect with the *Anabaena* enzyme and also with Fld. They indicate that partial reciprocal exclusion between $NADP^+$/H and both potential protein partners might be general among the photosynthetic forms of FNR.

Nonconservative mutations at the C-terminal position of pea and *Anabaena* FNR result in a drastic impairment of Fd(Fld)-dependent cytochrome *c* reductase activity (Table 4). The diaphorase reaction, which is independent of the protein carrier, was also inhibited by similar substitutions but to a lesser extent (*13*). In the latter case, inhibition was attributed to an abnormal increase of nucleotide affinity that prevented rapid turnover of the Michaelis complexes. Since the K_d (but not the K_m) values for Fd_{ox} or Fld_{ox} were also altered in the mutants (Tables 3 and 4), a similar mechanism could be invoked, in principle, to explain the slow-down of steady-state catalysis. If so, single-turnover events, as measured in rapid kinetics, should be unaffected by the replacements. ET from Fd_{rd} (Fld_{rd}) to FNR_{ox} was indeed equally fast in WT and mutant reductases, when measured by either flash photolysis (only for Fd, Table 5) or stopped-flow techniques. However, reduction of either Fd_{ox} or Fld_{ox} by FNR_{rd} was extensively blocked for some of the mutants, suggesting that replacement of the Tyr affected ET itself. The $E_{ox/rd}$ values determined for the *Anabaena* FNR mutants showed a slight tendency to shift to less negative values as compared to the WT enzyme, with the divergence being especially pronounced for the nonconservative Ser substitution (Table 2). The direction of the shifts appeared to be consistent with inhibition of ET from FNR_{rd} to Fd_{ox}, but we were unable to establish a correlation between the $E_{ox/rd}$ changes and the accompanying kinetic effects. ET was equally impaired in the Tyr303Phe and Tyr303Trp mutants, which have a very small shift, and in the Tyr303Ser mutant, which undergoes a much larger shift. The $E_{ox/rd}$ of the Ser-substituted cyanobacterial enzyme was close to that of free FAD (Table 2), as could be anticipated from removal of the phenol group that shields the isoalloxazine of the WT enzyme from bulk solvent. In addition, the Tyr303Ser mutant did not stabilize the semiquinone state during ET. Previous reports have shown that nonconservative replacements of a glutamate residue at position 301 (position 306 in pea) had a similar effect on $E_{ox/rd}$ and SQ stabilization, suggesting that the C-terminal region plays a general role in the modulation of these very important properties of FNR (*16*, *19*, *31*, *32*). The lack of a stable SQ could certainly cause highly impaired ET ability, compared to WT FNR, in those processes in which electrons are exchanged one at a time, namely, with Fd and Fld. Again, however, this explanation cannot be applied to the low activity of the Tyr303Phe and Tyr303Trp mutants, which display normal oxidoreduction intermediates (Table 2). Moreover, in these two mutants, especially in the Tyr303Trp one, impairment only takes place in the direction from FNR_{rd} to Fd_{ox}. WT FNR_{rd} is able to reduce Fd, despite the fact this should be a thermodynamically unfavorable process, partly due to the fact that the reduction potential of the Fd [2Fe-2S] cluster becomes less negative on complex formation, whereas that of FNR is more negative (*4*). Our results might indicate that when the Tyr303Phe and, especially, Tyr303Trp FNR mutants form complexes with Fd, changes in the reduction potentials do not occur, suggesting that the optimal complex for ET is not formed in these cases and that the Tyr residue contributed to create an adequate environment of the redox centers for efficient ET. This can be envisaged in the case of the Trp mutant, where Tyr has been replaced by a more bulky residue. As this amino acid is placed at the protein−protein interface (*11*), it may alter the orientation of the docking interaction.

In all the ET reactions between the different FNR forms and Fld, and despite the changes observed in reduction potential values, the driving force of the ET processes is still favorable for either reduction of Fld_{ox} to the semiquinone state by FNR_{rd} or of FNR_{ox} also to the semiquinone state by Fld_{rd}, i.e., the reactions we are able to follow by fast kinetic methods. When it is taken into account that the FNR/Fld interaction is proposed to be less specific than the FNR/Fd one (*1*), the single alteration of the terminal Tyr does not appear to alter the optimal FNR/Fld orientation to the same extent as the FNR/Fd one. Therefore, it is easy to understand that the mutants behaved more similarly to the WT FNR in their ability to exchange electrons with Fld. Once again, however, replacement of Tyr303 by either a Ser or a Trp prevents the formation of the most optimal complex for efficient ET.

It is conceivable that the properties displayed by C-terminal mutants of both pea and *Anabaena* reductases reflect the participation of the terminal Tyr in the mechanism of ET, either by providing an adequate environment for electron exchange between the corresponding prosthetic groups or by direct or indirect involvement in the protein-mediated ET.

FNR, *Anabaena PCC7119*	292	LKKAG-RWHVET**Y**	303
FNR, pea (leaf)	297	LKKAE-QWNVEV**Y**	308
FNR, corn (root)	305	LKKNK-QWHVEV**Y**	316
FPR, *E. coli*	239	PG----HMTAEH**Y**W	248
FPR, *A. vinelandii*	246	PG----DYLIER**A**FVEK	258
CYP450R, rat	665	KLMTKGRYSLDV**W**S	678
nNOS, rat	1383	RLRDDNRYHEDI**F**GV	1397
SiR, *E. coli*	588	LRVER-RYQRDV**Y**	599
NR, corn (root)	224	LDK---ACLVF	231
NR, corn (leaf)	614	MAN---SFVVF	621
Cb5R, rat	294	KE----RCFTF	300
PDR, *P. cepacia*	217	SG----TVHFES**F**GATNTNARE...	234

FIGURE 5: Sequence alignment of different pyridine nucleotide-dependent flavin oxidoreductases at the FNR Tyr303 region. C-Terminal sequences are aligned for all enzymes but PDR, which includes a ferredoxin-like C-terminal domain. Alignments have been obtained from structural superimposition of the corresponding three-dimensional structures. Numeration of aligned residues is shown at the left and right of each sequence. Hyphens denote gaps introduced to improve alignment. Structures used are as follows: *Anabaena* PCC7119 FNR (*8*); pea leaf FNR (*11*); corn root FNR (*43*); *E. coli* FNR (*41*); *A. vinelandii* FNR (*42*); rat CYP450R (*34*); rat neuronal NOS (*37*); *E. coli* SiR (*36*); corn root NR (*44*); corn leaf NR (*45*); rat Cb5R (*40*); *Pseudomonas cepacia* PDR (*38*). Tyr303 of *Anabaena* FNR, Tyr308 of pea FNR, and the residues equivalent in the other sequences are highlighted in boldface type.

The central theme of electron exchange between FNR and Fd (or Fld) relates to the motion of a single electron from one localized prosthetic group to another separated by several angstroms. In general, the electrons that are being shuttled in most physiological ET systems propagate from donor to acceptor without forming long-lived intermediate protein states; that is, the polypeptide backbone does not act as a conductor (*33*). Aromatic amino acids—Tyr in particular—occasionally behave as electron carriers, usually in the presence of a highly reactive redox partner, but the energies required to form such true protein intermediates far exceed those involved in the majority of biological redox reactions (*33*). Since donor and acceptor are seldom in close contact, the electron must tunnel along the insulating protein backbone to move between them. Consequently, the distance between the cofactors should be less than 17 Å to accomplish interprotein ET on a (sub)millisecond time scale at modest free energies (*33*). On the other hand, the redox centers must be sheltered by sufficient protein backbone to prevent accidental unproductive electron exchange with adventitious partners. This leaves ample opportunity for modulation of ET rates by the intervening amino acid residues.

The structures of FNR/Fd complexes conform to many of these features. The redox-active groups are placed asymmetrically, close to the surface of both proteins but partially buried within them, and are brought into close proximity during ET by patches of complementary charges that decorate the active sites (*9*, *10*). A detailed structure is not yet available for the corresponding complex of FNR with Fld. Modeling studies, with the NADPH−cytochrome P450 reductase structure as a blueprint, indicate that the flavin redox centers of the two proteins in the complex are close to each other, with the methyl groups of both flavins exposed to the solvent (*34*). In these two FNR complexes (with Fd and Fld), the C-terminal Tyr occupies a strategic position at the interface between the relevant prosthetic groups (*12*), establishing various interactions (hydrogen bonds, π orbital stacking, polar effects) with the redox-active centers and with other residues (*7*). These types of interactions strongly affect the efficiency of electron tunneling, as revealed by small-

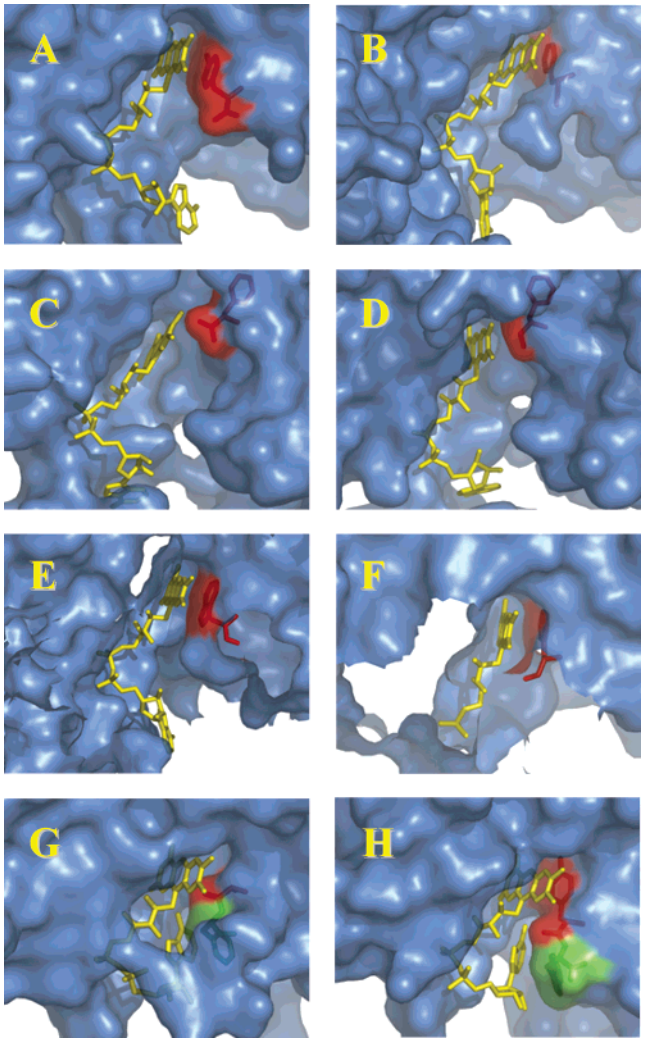

FIGURE 6: Structural arrangement of the FAD environment in different pyridine nucleotide-dependent flavin oxidoreductases: (A) FNR (PDB code 1QUE) (*8*); (B) NOS (1F20) (*37*); (C) NR (2CND) (*45*); (D) Cb5R (1I7P) (*40*); (E) CYP450R (1AMO) (*34*); (F) PDR (2PIA) (*38*); (G) *A. vinelandii* FNR (1A8P) (*42*); (H) *E. coli* FNR (1FDR) (*41*). Molecular surfaces are shown in blue, except for the surface contributed by selected residues, which is shown in red or green. FAD (FMN in PDR) is shown in yellow. Tyr303 of *Anabaena* FNR and equivalent residues (as marked in Figure 5) plus the C-terminal residues of nitrate reductase and Cb5R are shown in red. The Fd domain of PDR and the FMN-binding domain of CYP450R were removed for clarity. $NADP^+$/H-dependent reductases have a narrow cavity (panels A, B, and E) with an aromatic residue stacking against the isoalloxazine ring of FAD. PDR (panel F) is the only NADH-dependent reductase that shows this arrangement. The other NADH-dependent reductases (panels C and D) have a bigger cavity with the C-terminal residue pointing to the inner part of the protein. Bacterial FNRs (panels G and H) show a particular FAD conformation in which the FAD is bent by the stacking of an aromatic residue against the adenine moiety of FAD. The residues that make this stacking interaction with the adenine moiety of the FAD, Phe255 and Trp248 in *Azotobacter* and *E. coli* FNR, respectively, are shown in green. Figures were drawn with PyMOL (*46*).

molecule experiments (*35*). Thus, the present results show that the C-terminal Tyr plays a pivotal role in catalysis, not only through its effect on $NADP^+$/H affinity but also by stabilization of the SQ state of the bound FAD and by modulating the rate of hydride and electron transfer.

The function of this critical residue and the effects of the FAD environment on the kinetic properties of FNR can also

be envisaged from a comparison with other related enzymes. Many pyridine nucleotide-dependent flavin oxidoreductases have an aromatic residue at the position occupied by the C-terminal Tyr of FNR (*6*). Since this aromatic side chain lies parallel to the *re*-face of the flavin in FNR (Figure 6A), it was assumed that a similar position would be occupied by equivalent residues in other enzymes displaying similar properties. However, resolution of the three-dimensional structures of several of these proteins has shown that in some of them the aromatic side chain is not placed at the same position as the C-terminal Tyr in FNR and that new sequence alignments, based on the structural data, have to be proposed (Figure 5). The stacking interaction between an aromatic residue and the isoalloxazine ring in the $NAD(P)^+$/H binding site is present in most of the enzymes, including cytochrome P450 reductase (CYP450R) and sulfite reductase (SiR) (*34*, *36*) (Figure 6E). Other enzymes, such as nitric oxide synthase (NOS) and phthalate dioxygenase reductase (PDR), have an aromatic residue at this site but also contain an extension of the C-terminus (*37*, *38*) (Figure 6B,F). Finally, the stacking interaction is entirely absent in some enzymes that have an overall folding homologous to that of FNR. Such enzymes include nitrate reductase (NR) and cytochrome b_5 reductase (Cb5R), which clearly show an empty space at the corresponding position (*39*, *40*) (Figure 6C,D). Differences in the conformation of the C-terminal region can even be recognized between FNR proteins themselves. The reductase from *E. coli* has a Tyr residue equivalent to Tyr303, followed by a C-terminal Trp that stacks on the adenine ring of FAD (*41*), forcing a folded conformation of the prosthetic group that differs from the extended L structure observed in most other FNRs (Figure 6H). The position of the C-terminal Tyr in *Azotobacter vinelandii* FNR is, in turn, occupied by an Ala, whose carbonyl group interacts with N-10 of the flavin (*42*). This enzyme presents a four-residue extension of the C-terminus, relative to their chloroplast and cyanobacterial homologues. The first amino acid of this extra region, as in *E. coli* FNR, is an aromatic residue that favors adenine stacking and FAD folding (Figure 6G).

Since all of these enzymes are functional, it is tempting to suggest that the C-terminal Tyr plays a sensitive role but is by no means essential for catalysis. In this context, the relevance of that contribution could be gauged by considering that related enzymes that lack the Tyr at the FAD stacking position display turnover rates that are considerably slower than FNR forms that harbor typical C-terminal and FAD conformations. Optimization for catalytic efficiency in the chloroplast and cyanobacterial reductases might be related to the demands of the photosynthetic process that requires a very fast electron flow to sustain CO_2 fixation rates, whereas in organisms growing by heterotrophic metabolism or anoxygenic photosynthesis, FNR is more likely involved in pathways that proceed at a much slower pace (reviewed in ref *1*). As more FNR proteins from very distant organisms are isolated and characterized, these hypotheses could be probed in a systematic way.

REFERENCES

1. Carrillo, N., and Ceccarelli, E. A. (2003) Open questions in ferredoxin-$NADP^+$ reductase catalytic mechanism, *Eur. J. Biochem. 270*, 1900−1915.
2. Medina, M., and Gómez-Moreno, C. (2004) Interaction of ferredoxin-$NADP^+$ reductase with its substrates: optimal interaction for efficient electron transfer, *Photosynth. Res. 79*, 113−131.
3. Fillat, M. F., Sandman, G., and Gómez-Moreno, C. (1988) Flavodoxin from the nitrogen fixing cyanobacterium *Anabaena* PCC7119, *Arch. Microbiol. 150*, 160−164.
4. Hurley, J. K., Morales, R., Martínez-Julvez, M., Brodie, T. B., Medina, M., Gómez-Moreno, C., and Tollin, G. (2002) Structure−function relationships in *Anabaena* ferredoxin/ferredoxin-$NADP^+$ reductase electron transfer: insights from site-directed mutagenesis, transient absorption spectroscopy and X-ray crystallography, *Biochim. Biophys. Acta 1554*, 5−21.
5. Karplus, P. A., Daniels, M. J., and Herriott, J. R. (1991) Atomic structure of ferredoxin-$NADP^+$ reductase: prototype for a structurally novel flavoenzyme family, *Science 251*, 60−66.
6. Correll, C. C., Ludwig, M. L., Bruns, C. M., and Karplus, P. A. (1993). Phthalate dioxygenase reductase: a modular structure for electron transfer from pyridine nucleotides to [2Fe-2S], *Protein Sci. 2*, 2112−2133.
7. Bruns, C. M., and Karplus, P. A. (1995) Refined crystal structure of spinach ferredoxin reductase at 1.7 Å resolution: oxidized, reduced and 2′-phospho-5′-AMP bound states, *J. Mol. Biol. 247*, 125−145.
8. Serre, L., Vellieux, F. M., Medina, M., Gómez-Moreno, C., Fontecilla-Camps, J. C., and Frey, M. (1996) X-ray structure of the ferredoxin-$NADP^+$ reductase from the cyanobacterium *Anabaena* PCC 7119 at 1.8 Å resolution, and crystallographic studies of $NADP^+$ binding at 2.25 Å resolution, *J. Mol. Biol. 263*, 20−39.
9. Morales, R., Charon, M. H., Kachalova, G., Serre, L., Medina, M., Gómez-Moreno, C., and Frey, M. (2000) A redox-dependent interaction between two electron-transfer partners involved in photosynthesis, *EMBO Rep. 1*, 271−276.
10. Kurisu, G., Kusunoki, M., Katoh, E., Yamazaki, T., Teshima, K., Onda, Y., Kimata-Ariga, Y., and Hase, T. (2001) Structure of the electron-transfer complex between ferredoxin and ferredoxin-$NADP^+$ reductase, *Nat. Struct. Biol. 8*, 117−121.
11. Deng, Z., Aliverti, A., Zanetti, G., Arakaki, A. K., Ottado, J., Orellano, E. G., Calcaterra, N. B., Ceccarelli, E. A., Carrillo, N. and Karplus, P. A. (1999) A productive $NADP^+$ binding mode of ferredoxin-$NADP^+$ reductase revealed by protein engineering and crystallographic studies, *Nat. Struct. Biol. 6*, 847−853.
12. Hermoso, J. A., Mayoral, T., Faro, M., Gómez-Moreno, C., Sanz-Aparicio, J., and Medina, M. (2002) Mechanism of coenzyme recognition and binding revealed by crystal structure analysis of ferredoxin-$NADP^+$ reductase complexed with $NADP^+$, *J. Mol. Biol. 319*, 1133−1142.
13. Piubelli, L., Aliverti, A., Arakaki, A. K., Carrillo, N., Ceccarelli, E. A., Karplus, P. A., and Zanetti, G. (2000) Competition between C-terminal tyrosine and nicotinamide modulates pyridine nucleotide affinity and specificity in plant ferredoxin-$NADP^+$ reductase, *J. Biol. Chem. 275*, 10472−10476.
14. Batie, C. J., and Kamin, H. (1984) Ferredoxin-$NADP^+$ oxidoreductase. Equilibria in binary and ternary complexes with $NADP^+$ and ferredoxin, *J. Biol. Chem. 259*, 8832−8839.
15. Batie, C. J., and Kamin, H. (1984) Electron transfer by ferredoxin-$NADP^+$ reductase. Rapid-reaction evidence for participation of a ternary complex, *J. Biol. Chem. 259*, 11976−11985.
16. Medina, M., Martínez-Júlvez, M., Hurley, J. K., Tollin, G., and Gómez-Moreno, C. (1998) Involvement of glutamic acid 301 in the catalytic mechanism of ferredoxin-$NADP^+$ reductase from *Anabaena* PCC 7119, *Biochemistry 37*, 2715−2728.
17. Fillat, M. F., Borrias, W. E., and Weisbeek, P. J. (1991) Isolation and overexpression in *Escherichia coli* of the flavodoxin gene from *Anabaena* PCC 7119, *Biochem. J. 280*, 187−191.
18. Hurley, J. K., Weber-Main, A. M., Stankovich, M. T., Benning, M. M., Thoden, J. B., Vanhooke, J. L., Holden, H. M., Chae, Y. K., Xia, B., Cheng, H., Markley, J. L., Martínez-Júlvez, M., Gómez-Moreno, C., Schmeits, J. L., and Tollin, G. (1997) Structure−function relationships in *Anabaena* ferredoxin: correlations between X-ray crystal structures, reduction potentials, and rate constants of electron transfer to ferredoxin-$NADP^+$ reductase for site-specific ferredoxin mutants, *Biochemistry 36*, 11100−11117.
19. Faro, M., Gómez-Moreno, C., Stankovich, M., and Medina, M. (2002) Role of critical charged residues in reduction potential modulation of ferredoxin-$NADP^+$ reductase, *Eur. J. Biochem. 269*, 2656−2661.

20. Pueyo, J. J., Gómez-Moreno, C., and Mayhew, S. G. (1991) Oxidation−reduction potentials of ferredoxin-NADP$^+$ reductase and flavodoxin from *Anabaena* PCC 7119 and their electrostatic and covalent complexes, *Eur. J. Biochem. 202*, 1065−71.
21. Mayhew, S. G. (1999) Potentiometric measurement of oxidation-reduction potentials, in *Flavoprotein Protocols* (Chapman, S. K., and Reid, G. A., Eds.) pp 49−59, Humana Press, Totowa, NJ.
22. Casaus, J. L., Navarro, J. A., Hervas, M., Lostao, A., De la Rosa, M. A., Gómez-Moreno, C., Sancho, J., and Medina, M. (2002) *Anabaena* sp. PCC 7119 flavodoxin as electron carrier from photosystem I to ferredoxin-NADP$^+$ reductase. Role of Trp(57) and Tyr(94), *J. Biol. Chem. 277*, 22338−22344.
23. Tollin, G. (1995) Use of flavin photochemistry to probe intraprotein and interprotein electron-transfer mechanisms, *J. Bioenerg. Biomembr. 27*, 303−309.
24. Hurley, J. K., Fillat, M. F., Gómez-Moreno, C., and Tollin, G. (1996) Electrostatic and hydrophobic interactions during complex formation and electron transfer in the ferredoxin-NADP$^+$ reductase system from *Anabaena*, *J. Am. Chem. Soc. 118*, 5526−5531.
25. Lostao, A., Gómez-Moreno, C., Mayhew, S. G., and Sancho, J. (1997) Differential stabilization of the three FMN redox forms by tyrosine 94 and tryptophan 57 in flavodoxin from *Anabaena* and its influence on the redox potentials, *Biochemistry 36*, 14334−14344.
26. Clark, W. M., and Lowe, H. J. (1956) Studies on oxidation−reduction. XXIV. Oxidation−reduction potentials of flavin adenine dinucleotide, *J. Biol. Chem. 221*, 983−992.
27. Simondsen, R. P., and Tollin, G. (1983). Transient kinetics of redox reactions of flavodoxin: effects of chemical modification of the flavin mononucleotide prosthetic group on the dynamics of intermediate complex formation and electron transfer, *Biochemistry 22*, 3008−3016.
28. Hurley, J. K., Fillat, M. F., Gómez-Moreno, C., and Tollin, G. (1995) Structure−function relationships in the ferredoxin/ferredoxin:NADP$^+$ reductase system from *Anabaena*, *Biochimie 77*, 539−48.
29. Dorowski, A., Hofmann, A., Steegborn, C., Boicu, M., and Huber, R. (2001) Crystal structure of paprika ferredoxin-NADP$^+$ reductase. Implications for the electron-transfer pathway, *J. Biol. Chem. 276*, 9253−9263.
30. Medina, M., Bazo, J. I., Fillat, M. F., and Gómez-Moreno, C. (1993) Structure predictions of ferredoxin-NADP$^+$ reductase from the cyanobacterium *Anabaena sp* PCC 7119, *Protein Seq. Data Anal. 5*, 247−252.
31. Aliverti, A., Deng, Z., Ravasi, D., Piubelli, L., Karplus, P. A., and Zanetti, G. (1998) Probing the function of the invariant glutamyl residue 312 in spinach ferredoxin-NADP$^+$ reductase, *J. Biol. Chem. 273*, 34008−34015.
32. Mayoral, T., Medina, M., Sanz-Aparicio, J., Gómez-Moreno, C., and Hermoso, J. A. (2000) Structural basis of the catalytic role of Glu301 in *Anabaena* PCC 7119 ferredoxin-NADP$^+$ reductase revealed by X-ray crystallography, *Proteins: Struct., Funct., Genet. 38*, 60−69.
33. Bendall, D. S., Ed. (1996) *Protein Electron Transfer*, Bioscientific Publishers, Oxford, U.K.
34. Wang, M., Roberts, D. L., Paschke, R., Shea, T. M., Masters, B. S., and Kim, J. J. (1997). Three-dimensional structure of NADPH−cytochrome P450 reductase: prototype for FMN- and FAD-containing enzymes, *Proc. Natl. Acad. Sci. U.S.A. 94*, 8411−8416.
35. de Rege, P. J., Williams, S. A. and Therien, M. J. (1995) Direct evaluation of electronic coupling mediated by hydrogen bonds: implications for biological electron transfer, *Science 269*, 1409−1413.
36. Gruez, A., Pignol, D., Zeghouf, M., Coves, J., Fontecave, M., Ferrer, J. L., and Fontecilla-Camps, J. C. (2000) Four crystal structures of the 60 kDa flavoprotein monomer of the sulfite reductase indicate a disordered flavodoxin-like module, *J. Mol. Biol. 299*, 199−212.
37. Zhang, J., Martasek, P., Paschke, R., Shea, T., Siler Masters, B. S., and Kim, J. J. (2001) Crystal structure of the FAD/NADPH-binding domain of rat neuronal nitric-oxide synthase. Comparisons with NADPH−cytochrome P450 oxidoreductase, *J. Biol. Chem. 276*, 37506−37513.
38. Correll, C. C., Batie, C. J., Ballou, D. P., and Ludwig, M. L. (1992) Phthalate dioxygenase reductase: a modulas structure for electron transfer from pyridine nucleotides to [2Fe-2S], *Science 258*, 1604−1610.
39. Lu, G., Lindqvist, Y., Schneider, G., Dwivedi, U., and Campbell, W. (1995) Structural studies on corn nitrate reductase: refined structure of the cytochrome *b* reductase fragment at 2.5 Å, its ADP complex and an active-site mutant and modeling of the cytochrome *b* domain, *J. Mol. Biol. 248*, 931−948.
40. Bewley, M. C., Marohnic, C. C., and Barber, M. J. (2001) The structure and biochemistry of NADH-dependent cytochrome *b*5 reductase are now consistent, *Biochemistry 40*, 13574−13582.
41. Ingelman, M., Bianchi, V., and Eklund, H. (1997) The three-dimensional structure of flavodoxin reductase from *Escherichia coli* at 1.7 Å resolution. *J. Mol. Biol. 268*, 147−157.
42. Sridhar Prasad, G., Kresge, N., Muhlberg, A. B., Shaw, A., Jung, Y. S., Burgess, B. K., and Stout, C. D. (1998) The crystal structure of NADPH:ferredoxin reductase from *Azotobacter vinelandii*, *Protein Sci. 7*, 2541−2549.
43. Aliverti, A., Faber, R., Finnerty, C. M., Ferioli, C., Pandini, V., Negri, A., Karplus, P. A., and Zanetti, G. (2001) Biochemical and crystallographic characterization of ferredoxin-NADP$^+$ reductase from nonphotosynthetic tissues, *Biochemistry 40*, 14501−14508.
44. Long, D. M., Oaks, A., and Rothstein, S. J. (1992) Regulation of maize root nitrate reductase mRNA levels, *Physiol. Plant. 85*, 561−566.
45. Lu, G., Campbell, W. H., Schneider, G., and Lindqvist, Y. (1994) Crystal structure of the FAD-containing fragment of corn nitrate reductase at 2.5 Å resolution: relationship to other flavoprotein reductases, *Structure 2*, 809−821.
46. DeLano, W. L. (2002) The PyMOL Molecular Graphics System, DeLano Scientific, San Carlos, CA.

BI049858H